PHASE PORTRAITS OF PLANAR PIECEWISE LINEAR REFRACTING SYSTEMS: FOCUS-SADDLE CASE

SHIMIN LI[1] AND JAUME LLIBRE[2]

Abstract. This paper deal with planar piecewise linear refracting systems with a straight line of separation. Using the Poincaré compactification, we provide the classification of the phase portraits in the Poincaré disc of piecewise linear refracting systems with focus-saddle dynamics.

1. Introduction

Global phase portraits are an invaluable tool in studying the long dynamical behaviour of differential systems. They reveals information such as whether an attractor, a repellor or a limit cycle is present for a given parameter value. Hence the global phase portraits analysis is the one of most important problems in the qualitative theory of differential systems.

The possibilities of topological distinct phase portraits for a general polynomial differential system are huge, it is expected that the quadratic polynomial differential systems have more than 2000 topological distinct phase portraits. As far as we know, most of known results about global phase portraits are mainly deal with smooth differential systems, see for instance [1, 2, 6, 7, 8, 9, 11, 15, 18, 25].

Many real-world systems involve a discontinuity or sudden change, such as friction in mechanical systems [10] and switching in electrical circuits [29]. Smooth differential systems generally do not provide ideal mathematical models for such situations. It becomes necessary to incorporate a non-smooth component into the model. Often this yields a piecewise smooth differential systems [3, 4].

In order to state precisely our results we introduce first some notations and definitions. Let us denote by Ω^r the sets of C^r planar vector fields ($r > 1$), The set of planar piecewise smooth vector fields given by

$$Z(x,y) = \begin{cases} X(x,y), & f(x,y) < 0, \\ Y(x,y), & f(x,y) > 0, \end{cases} \tag{1.1}$$

where $X, Y \in \Omega^r$, and the smooth function f have $0 \in \mathbb{R}$ as a regular value (i.e. $\nabla f(p) \neq 0$, for any $p \in f^{-1}(0)$).

We say that $p \in \mathbb{R}^2$ is a *visible* (resp. *invisible*) equilibrium of X if $X(p) = 0$ and $f(p) < 0$ (resp. $f(p) > 0$). Similarly, p is a *visible* (resp. *invisible*) equilibrium of Y if $Y(p) = 0$ and $f(p) > 0$ (resp. $f(p) < 0$).

2010 *Mathematics Subject Classification.* 34C37, 34C07, 37G15.

Key words and phrases. Phase portraits; Refracting systems; Limit cycle.

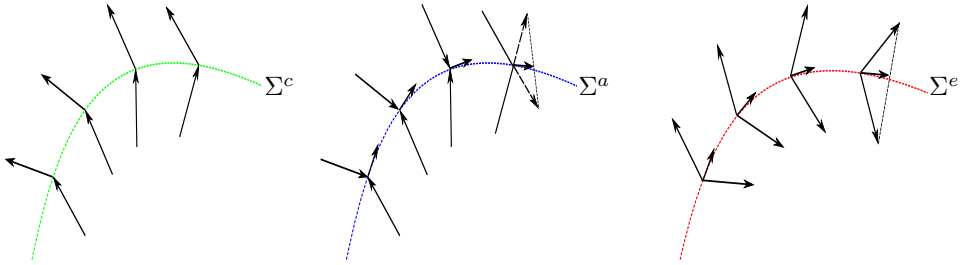

1.1 crossing region 1.2 attracting region 1.3 escaping region

FIGURE 1. Definition of the vector field on Σ.

Definition 1.1. *The discontinuous set $\Sigma = f^{-1}(0)$ can be divided into three open regions:*

(i) *Crossing region $\Sigma^c = \{p \in \Sigma | Xf(p)Yf(p) > 0\}$, see Fig.1.1;*
(ii) *Attracting region $\Sigma^a = \{p \in \Sigma | Xf(p) > 0, Yf(p) < 0\}$, see Fig.1.2;*
(iii) *Escaping region $\Sigma^e = \{p \in \Sigma | Xf(p) < 0, Yf(p) > 0\}$, see Fig.1.3.*

where $Xf(p) = \langle \nabla f(p), X(p) \rangle$.

The boundary of the above regions are called $\Sigma-$*tangential points*, that is $\Sigma^t = \{p \in \Sigma | Xf(p)Yf(p) = 0\}$. The simplest tangency is the fold point, which is defined as follows.

Definition 1.2. *$p \in \Sigma$ is a fold point of X if $Xf(p) = 0$ and $X^2 f(p) \neq 0$. Here $X^2 f = X(Xf)$. The fold is visible if $X^2 f(p) > 0$ and it is invisible if $X^2 f(p) < 0$. Analogously, a fold point $p \in \Sigma$ of Y satisfies $Yf(p) = 0$ and $Y^2 f(p) \neq 0$, and it is visible if $Y^2 f(p) < 0$ and invisible if $Y^2 f(p) > 0$.*

We are interested in a special kind of discontinuous differential systems which are known as refracting systems [5, 26]. The precise definition is given as follows.

Definition 1.3. *If $Xf(p) = Yf(p)$ for any $p \in \Sigma$, then systems (1.1) are known as refracting systems.*

The most simplest piecewise smooth differential systems are planar piecewise linear systems with a straight line of separation. In 2012, Freire, Ponce and Torres[14] deduced planar piecewise linear systems into Liénard canonical forms

$$\begin{pmatrix} \dot{x} \\ \dot{y} \end{pmatrix} = \begin{cases} \begin{pmatrix} T^- & -1 \\ D^- & 0 \end{pmatrix} \begin{pmatrix} x \\ y \end{pmatrix} - \begin{pmatrix} 0 \\ a^- \end{pmatrix}, & x < 0, \\ \begin{pmatrix} T^+ & -1 \\ D^+ & 0 \end{pmatrix} \begin{pmatrix} x \\ y \end{pmatrix} - \begin{pmatrix} -b \\ a^+ \end{pmatrix}, & x > 0, \end{cases} \tag{1.2}$$

where $T^{\pm}$ and $D^{\pm}$ are denote the traces and determinants of the left (right) subsystems, respectively. We call systems (1.2) with $x < 0$ (resp. $x > 0$) the left (resp. right) subsystems for convenience.

If $b = 0, a^- = a^+$, then systems (1.2) become continuous systems. In 1990, Lum and Chua[23] conjectured that planar piecewise linear continuous systems (1.2) have at most one limit cycle, and this conjecture was proved by Freire, etc. [13].

Recently, Li and Llibre [19] provided the global phase portraits in the poincaré dics of continuous systems (1.2).

For the discontinuous systems (1.2), most of the known results are concerned with the lower bounds of the number of limit cycles, see [21, 22] and the references therein. According to the equilibrium of left and right subsystems (1.2), we can classify systems (1.2) into FF, FS, FN, SS, SN, NN cases, where F, S, N denote focus/center, saddle and node respectively.

If $b = 0$, then systems (1.2) become refracting systems by Definition 1.3. Piecewise linear refracting systems (1.2) have been studied in several papers [14, 16, 17, 26, 27, 28], all of these results show that piecewise linear refracting systems (1.2) have at most one limit cycle.

In the present paper, we investigate the global phase portraits of planar piecewise linear refracting systems of the focus-saddle type. Without loss of generality, we assume that the left subsystems of (1.2) have a focus and the right subsystems of (1.2) have a saddle. We introduce some auxiliary parameters as follows:

$$\omega_L = \frac{\sqrt{4D^- - (T^-)^2}}{2}, \quad \gamma_L = \frac{T^-}{2\omega_L},$$
$$\omega_R = \frac{\sqrt{(T^+)^2 - 4D^+}}{2}, \quad \gamma_R = \frac{T^+}{2\omega_R}.$$

Do the change of variables $x = \dfrac{\bar{x}}{\omega_L}, y = \bar{y}, t = \dfrac{\bar{t}}{\omega_L}$ for $x < 0$ and $x = \dfrac{\bar{x}}{\omega_R}, y = \bar{y}, t = \dfrac{\bar{t}}{\omega_R}$ for $x > 0$, after dropping tildes, the canonical forms (1.2) with $b = 0$ can be written as

$$\begin{pmatrix} \dot{x} \\ \dot{y} \end{pmatrix} = \begin{cases} \begin{pmatrix} 2\gamma_L & -1 \\ \gamma_L^2 + 1 & 0 \end{pmatrix} \begin{pmatrix} x \\ y \end{pmatrix} - \begin{pmatrix} 0 \\ \alpha_L \end{pmatrix}, & x < 0, \\ \begin{pmatrix} 2\gamma_R & -1 \\ \gamma_R^2 - 1 & 0 \end{pmatrix} \begin{pmatrix} x \\ y \end{pmatrix} - \begin{pmatrix} 0 \\ \alpha_R \end{pmatrix}, & x > 0, \end{cases} \tag{1.3}$$

where $\gamma_L \neq 0$ and $|\gamma_R| < 1$.

We say that two phase portraits of Z_1 and Z_2 of systems (1.1) are *topologically equivalent* if there exists a homeomorphism $h : \mathbb{D}^2 \to \mathbb{D}^2$ such that it takes orbits of Z_1 onto orbits of Z_2 either preserving the orientation, or reversing the orientation of all orbits; also the discontinuous sets are preserved by the homeomorphism h.

Without loss of generality we assume that $\gamma_L > 0$, otherwise doing the change of variables $X = x, Y = -y, T = -t$, we change $\gamma_L < 0$ into the former one.

Our main result is the following one:

Theorem 1.4. *The phase portrait on the Poincaré disc of refracting system* (1.3) *with* $\gamma_L > 0, |\gamma_R| < 1$*, is topologically equivalent to one of the 18 phase portraits described in Figure 2.*

The rest of the paper is organized as follows. In section 2 we give a preliminary introduction for poincaré compactification, which is a crucial tool to investigate the

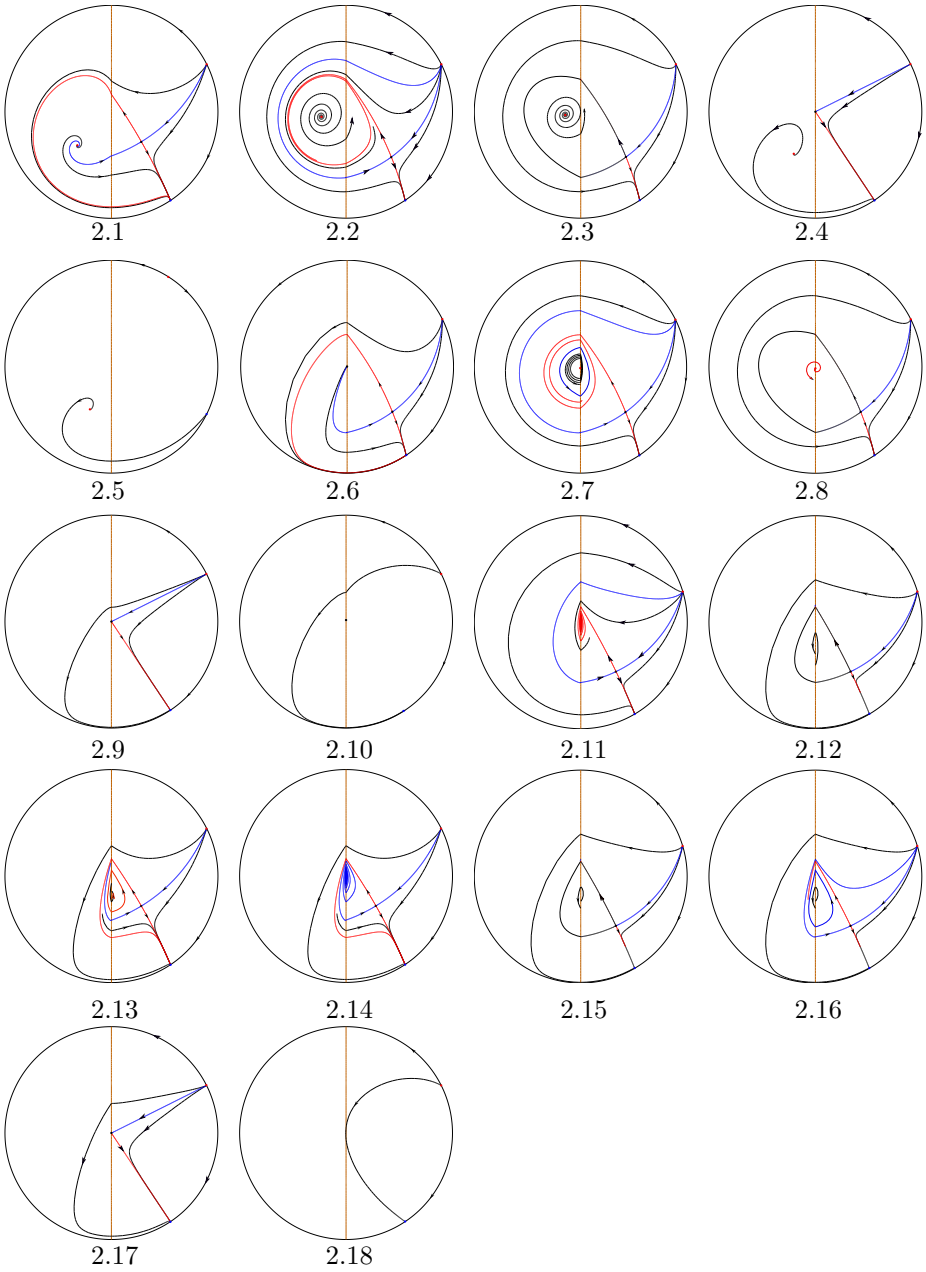

FIGURE 2. Global phase portraits of refracting systems (1.3)

global phase portraits of our systems. In section 3 we study the number of limit cycles of systems (1.3). The proof of Theorem 1.4 will be given in section 4.

2. Singular points

2.1. **Poincaré compactification.** For a given polynomial differential system

$$\frac{dx}{dt} = P(x,y), \qquad \frac{dy}{dt} = Q(x,y), \tag{2.1}$$

of degree $d = \max\{\deg(P), \deg(Q)\}$. Let $\mathcal{X} = (P,Q)$ be the vector field associated to system (2.1).

We call $\mathbb{S}^2 = \{\mathbf{s} = (s_1, s_2, s_3) \in \mathbb{R}^3 : s_1^2 + s_2^2 + s_3^2 = 1\}$ the *Poincaré sphere*. The *Poincaré compactified vector field* $p(\mathcal{X})$ *corresponding to* $\mathcal{X}$ is an analytic vector field induced on $\mathbb{S}^2$ as follows.

First we take $\mathbb{R}^2$ as the plane in $\mathbb{R}^3$ defined by $(x, y, 1) \in \mathbb{R}^3$, and then project each point $(x, y, 1)$ in two points of the Poincaré sphere $\mathbb{S}^2$ using the straight line through $(x, y, 1)$ and the origin $(0, 0, 0)$. It is obvious that the equator $\mathbb{S}^1 = \{\mathbf{s} \in \mathbb{S}^2, s_3 = 0\}$ corresponds to the infinity of $\mathbb{R}^2$. So we have two copies of the vector field $\mathcal{X}$ on the Poincaré sphere $\mathbb{S}^2$, one in the open northern hemisphere $\mathbb{S}^- = \{\mathbf{s} \in \mathbb{S}^2 : s_3 > 0\}$, and the other in the open southern hemisphere $\mathbb{S}^+ = \{\mathbf{s} \in \mathbb{S}^2 : s_3 < 0\}$. This vector field $\mathcal{X}'$ on $\mathbb{S}^2 \setminus \mathbb{S}^1$ can be extended to a vector field $p(\mathcal{X})$ defined in the whole $\mathbb{S}^2$ by multiplying $\mathcal{X}'$ by s_3^d.

For studying the Poincaré sphere we use the following six local charts

$$U_i = \{\mathbf{s} \in \mathbb{S}^2 : \ s_i > 0\}, \ V_i = \{\mathbf{s} \in \mathbb{S}^2 : \ s_i < 0\}, \quad i = 1, 2, 3, \tag{2.2}$$

with the corresponding diffeomorphisms $\varphi_k : U_k \to \mathbb{R}^2$ and $\psi_k : V_k \to \mathbb{R}^2$ defined by $\varphi_k(\mathbf{s}) = -\psi_k(\mathbf{s}) = (s_m/s_k, s_n/s_k) = (u, v)$ for $m < n$ and $m, n \neq k$. Note that the coordinates (u, v) play a different role in each local chart.

The expression of $p(\mathcal{X})$ in the local chart U_1 is

$$\frac{du}{dt} = v^d\Big[-uP\left(\frac{u}{v}, \frac{1}{v}\right) - uQ\left(\frac{u}{v}, \frac{1}{v}\right)\Big], \qquad \frac{dv}{dt} = -v^{d+1}Q\left(\frac{u}{v}, \frac{1}{v}\right). \tag{2.3}$$

The expression of $p(\mathcal{X})$ in the local chart U_2 is

$$\frac{du}{dt} = v^d\Big[-uP\left(\frac{1}{v}, \frac{u}{v}\right) + Q\left(\frac{1}{v}, \frac{u}{v}\right)\Big], \qquad \frac{dv}{dt} = -v^{d+1}P\left(\frac{1}{v}, \frac{u}{v}\right). \tag{2.4}$$

In the charts V_i for $i = 1, 2$ the expressions of $p(\mathcal{X})$ are the same in U_i but multiplied by $(-1)^{d-1}$.

The expression of $p(\mathcal{X})$ in the local charts $U_3 \equiv V_3$ are just

$$\frac{du}{dt} = P(u,v), \quad \frac{dv}{dt} = Q(u,v). \tag{2.5}$$

For studying the phase portrait of a polynomial differential system (2.1), we just need to study its Poincaré compactification $p(\mathcal{X})$ restricted to the closed northern hemisphere. We do the orthogonal projection $\pi(s_1, s_2, s_3) = (s_1, s_2)$ of the closed northern hemisphere onto the Poincaré disc $\mathbb{D}^2 = \{s_1^2 + s_2^2 \leqslant 1, s_3 = 0\}$ for drawing the phase portrait.

It is obvious that the finite equilibria of system (2.1) are the equilibria in the interior of $\mathbb{D}^2$, and they can be studied using U_3. The infinite equilibria of system

(2.1) are the equilibria of $p(\mathcal{X})$ in the boundary of $\mathbb{D}^2$. Note that for studying the infinite equilibria it suffices to look for the ones at the local charts $U_1|_{v=0}$ and $V_1|_{v=0}$, and at the origin of the local charts U_2 and V_2.

For more details on the poincaré compactification, see Chapter 5 of [12].

2.2. **Chart $\mathbf{U}_1$.** Let $x = \dfrac{1}{v}, y = \dfrac{u}{v}, v > 0$, then systems (1.3) become

$$\begin{cases} \dfrac{du}{dt} = u^2 - 2\gamma_R u - \alpha_R v + \gamma_R^2 - 1, \\ \dfrac{dv}{dt} = v(u - 2\gamma_R). \end{cases} \tag{2.6}$$

Since the equilibrium of systems (2.6) with $v = 0$ correspondence with the infinite equilibrium of systems (1.3) in chart U_1, we have the following results directly.

Proposition 2.1. *For systems* (1.3) *with* $|\gamma_R| < 1$*, then systems* (1.3) *have two infinite equilibrium:* $E_1 = (\gamma_R - 1, 0)$ *is a stable node, and* $E_2 = (\gamma_R + 1, 0)$ *is an unstable node.*

2.3. **Chart $\mathbf{V}_1$.** Let $x = \dfrac{1}{v}, y = \dfrac{u}{v}, v < 0$, then systems (1.3) become

$$\begin{cases} \dfrac{du}{dt} = u^2 - 2\gamma_L u - \alpha_L v + \gamma_L^2 + 1, \\ \dfrac{dv}{dt} = v(u - 2\gamma_L). \end{cases} \tag{2.7}$$

It is obvious that systems (1.3) have no infinite equilibrium in chart V_1 because systems (2.7) have no equilibrium when $v = 0$.

2.4. **Charts $\mathbf{U}_2$ and V_2.** Let $x = \dfrac{u}{v}, y = \dfrac{1}{v}$, then systems (1.3) become

$$\begin{cases} \dfrac{du}{dt} = (1 - \gamma_R^2)u^2 + \alpha_R uv + 2\gamma_R u - 1, \\ \dfrac{dv}{dt} = v(\alpha_R v + u - \gamma_R^2 u). \end{cases} \tag{2.8}$$

with $uv \geqslant 0$, and

$$\begin{cases} \dfrac{du}{dt} = -(1 + \gamma_L^2)u^2 + \alpha_L uv + 2\gamma_L u - 1, \\ \dfrac{dv}{dt} = v(\alpha_L v - u - \gamma_L^2 u). \end{cases} \tag{2.9}$$

with $uv \leqslant 0$.

Since $(0, 0)$ is neither a singular point of system (2.8) nor a singular point of system (2.9), the origins of U_2 and V_2 are not infinite equilibrium.

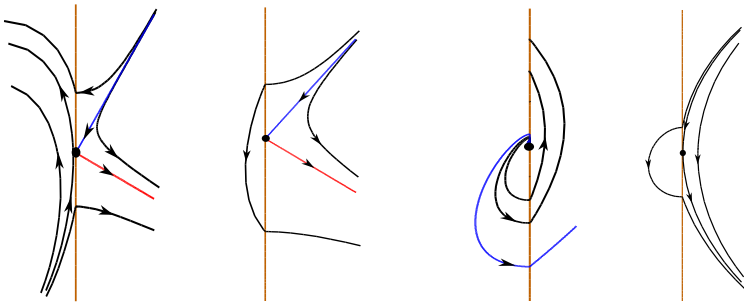

*Fig.*3.1 *Fig.*3.2 *Fig.*3.3 *Fig.*3.4

FIGURE 3. Phase portraits for boundary equilibrium of systems (1.3).

2.5. **Chart $\mathbf{U}_3$.** Let

$$P_L = \left(\frac{\alpha_L}{\gamma_L^2+1}, \frac{2\alpha_L\gamma_L}{\gamma_L^2+1}\right), \quad P_R = \left(\frac{\alpha_R}{\gamma_R^2-1}, \frac{2\alpha_R\gamma_R}{\gamma_R^2-1}\right). \tag{2.10}$$

Proposition 2.2. *For systems* (1.3) *with* $\gamma_L > 0$ *and* $|\gamma_R| < 1$ *the following statements hold.*

(I) *If* $\alpha_L < 0$ *and* $\alpha_R < 0$, *then systems* (1.3) *have two equilibrium:* P_L *is an unstable focus;* P_R *is a saddle.*
(II) *If* $\alpha_L < 0$ *and* $\alpha_R = 0$, *then systems* (1.3) *have two equilibrium:* P_L *is a unstable focus;* $O = (0,0)$ *is a boundary equilibrium which is known as visible fold-saddle, see Fig.3.1.*
(III) *If* $\alpha_L < 0$ *and* $\alpha_R > 0$, *then systems* (1.3) *have one equilibrium* P_L *which is an unstable focus.*
(IV) *If* $\alpha_L > 0$ *and* $\alpha_R > 0$, *then systems* (1.3) *have no equilibrium.*
(V) *If* $\alpha_L > 0$ *and* $\alpha_R = 0$, *then systems* (1.3) *have a boundary equilibrium* $O = (0,0)$ *which is known as invisible fold-saddle, see Fig.3.2.*
(VI) *If* $\alpha_L > 0$ *and* $\alpha_R < 0$, *then systems* (1.3) *have one equilibrium* P_R, *which is a saddle.*
(VII) *If* $\alpha_L = 0$ *and* $\alpha_R < 0$ *then systems* (1.3) *have two equilibrium:* P_R *is a saddle;* $O = (0,0)$ *is a boundary equilibrium, see Fig.3.3.*
(IV) *If* $\alpha_L = 0$ *and* $\alpha_R = 0$, *then systems* (1.3) *have a boundary equilibrium* $O = (0,0)$, *see Fig.3.2.*
(IX) *If* $\alpha_L = 0$ *and* $\alpha_R > 0$, *then systems* (1.3) *have a boundary equilibrium* $O = (0,0)$, *see Fig.3.4.*

Proof. The qualitative analysis of the visible equilibrium are directly, so we omit it here. In the following we just need to analyze the phase portraits of the boundary equilibrium $O(0,0)$.

(II) For the case $\alpha_L < 0, \alpha_R = 0$. In the region $x > 0$, the right subsystems of (1.3) is governed by the saddle $(0,0)$. It has two invariant straight lines $y = (\gamma_R - 1)x$ and $y = (\gamma_R + 1)x$. While in the region $x < 0$, the dynamics of left subsystems of (1.3) are governed by a visible focus P_L. From the above analysis, the phase portraits of the boundary equilibrium $(0,0)$ is Fig.3.1.

(V) For the case $\alpha_L > 0, \alpha_R = 0$. In the region $x > 0$, the dynamics of the origin is the same as case (II). While in the region $x < 0$, the dynamics of left subsystems of (1.3) are governed by an invisible focus P_L. From the above analysis, the phase portraits of the boundary equilibrium $(0, 0)$ is Fig.3.2.

(VII) For the case $\alpha_L = 0, \alpha_R < 0$. In the region $x < 0$, the dynamics of left subsystems of (1.3) are governed by the focus $O(0, 0)$. While in the region $x > 0$, the right subsystems of (1.3) have a visible saddle. Hence the phase portraits of the boundary equilibrium $(0, 0)$ is Fig.3.3.

(IV) For the case $\alpha_L = 0, \alpha_R = 0$. The phase portraits of the boundary equilibrium $(0, 0)$ is the same as Fig.3.2.

(IX) For the case $\alpha_L = 0, \alpha_R > 0$. In the region $x < 0$, the dynamics of left subsystems of (1.3) is the same as case (VII). In the region $x > 0$, the right subsystems of (1.3) have an invisible saddle. Hence the phase portraits of the boundary equilibrium $(0, 0)$ is Fig.3.4.

□

3. limit cycles

This section devote to study the limit cycles, which is very important for the investigation of global phase portraits of systems (1.3). According to the proposition 3.7 of [14] and note that $b = 0$, then a necessary condition for the existence of limit cycles is $\gamma_L\gamma_R < 0$. In order to have limit cycles it is obvious that the saddle P_R should visible, that is $\alpha_R < 0$.

In the paper [26], the authors obtain the uniqueness of limit cycles of systems (1.3) when the finite equilibrium are visible.

Theorem 3.1. *Consider refracting systems* (1.3) *with* $\gamma_L > 0, \gamma_R < 0$ *and* $\alpha_L < 0, \alpha_R < 0$. *If we define the values*

$$V_\pm = \pm e^{\gamma_L \theta_\pm} \sqrt{1 + [\gamma_L + \rho(\gamma_R \pm 1)]^2}, \tag{3.1}$$

with

$$\rho = \frac{\mu_R}{\mu_L} \frac{\omega_L(1 + \gamma_L^2)}{\omega_R(1 - \gamma_R^2)}, \tag{3.2}$$

and

$$\theta_\pm = \pm 2 \arctan\left(\sqrt{1 + [\gamma_L + \rho(\gamma_R \pm 1)]^2} \mp [\gamma_L + \rho(\gamma_R \pm 1)] \right). \tag{3.3}$$

Then the following statements hold.

(a) *If* $e^{\pi\gamma_L} V_+ + V_- < 0$, *then the unstable focus* P_L *is surrounded by one stable limit cycle.*
(b) *If* $e^{\pi\gamma_L} V_+ + V_- = 0$, *then the unstable focus* P_L *is surrounded by a homoclinic orbit and there are no limit cycle.*
(a) *If* $e^{\pi\gamma_L} V_+ + V_- > 0$, *then the the system does not have either limit cycles or homoclinic connections.*

For the remain case $\alpha_L \geqslant 0, \alpha_R < 0$, we have the following result.

Theorem 3.2. *Assume that $\gamma_L > 0, \gamma_R < 0$ and $\alpha_L \geqslant 0, \alpha_R < 0$, then refracting systems* (1.3) *have at most one limit cycle.*

Proof. If $\alpha_L > 0$ then the left subsystems of (1.3) have an invisible focus, and an equilibrium on Σ when $\alpha_L = 0$. Do the change of variables

$$X = 2\gamma_L x - y, \quad Y = x, \quad \text{if } x < 0,$$

$$X = 2\gamma_R x - y, \quad Y = x, \quad \text{if } x > 0,$$

then the refracting systems (1.3) become

$$\begin{pmatrix} \dot{X} \\ \dot{Y} \end{pmatrix} = \begin{cases} \begin{pmatrix} 2\gamma_L & -(\gamma_L^2+1) \\ 1 & 0 \end{pmatrix} \begin{pmatrix} X \\ Y \end{pmatrix} + \begin{pmatrix} \alpha_L \\ 0 \end{pmatrix} & \text{if } Y < 0, \\ \begin{pmatrix} 2\gamma_R & -(\gamma_R^2-1) \\ 1 & 0 \end{pmatrix} \begin{pmatrix} X \\ Y \end{pmatrix} + \begin{pmatrix} \alpha_R \\ 0 \end{pmatrix} & \text{if } Y > 0. \end{cases} \tag{3.4}$$

It is easy to check that $(0,0)$ is the unique $\Sigma-$monodromic singularity of systems (3.4). According with Theorem 1.1 of [24], systems (3.4) have at most one limit cycle because $\gamma_R\gamma_L < 0$. □

4. Proof of Theorem 1.4

We divide the proof of Theorem 1.4 into two cases.

4.1. $\gamma_R < 0$.

Proposition 4.1. *The phase portrait of refracting systems (1.3) with $\gamma_L > 0$ and $\gamma_R < 0$ is topologically equivalent to*

(I) *the ones of Fig.2.1, Fig.2.2 or Fig.2.3 if $\alpha_L < 0, \alpha_R < 0$;*
(II) *Fig.2.4 if $\alpha_L < 0$ and $\alpha_R = 0$;*
III) *Fig.2.5 if $\alpha_L < 0$ and $\alpha_R > 0$;*
(IV) *the ones of Fig.2.6, Fig.2.7 or Fig.2.8 if $\alpha_L = 0$ and $\alpha_R < 0$;*
(V) *Fig.2.9 if $\alpha_L = 0$ and $\alpha_R = 0$;*
(VI) *Fig.2.10 if $\alpha_L = 0$ and $\alpha_R > 0$;*
(VII) *the ones of Fig.2.11, Fig.2.12, Fig.2.13, Fig2.14, Fig.2.15 or Fig2.16 if $\alpha_L > 0$ and $\alpha_R < 0$;*
(VIII) *Fig.2.17 if $\alpha_L > 0$ and $\alpha_R = 0$;*
(XI) *Fig.2.18 if $\alpha_L > 0$ and $\alpha_R > 0$;*

Proof. Proposition 2.1 shows that systems (1.3) have two infinite equilibrium: E_1 is a stable node, and E_2 is an unstable node. From Theorems 3.1 and 3.2 we know that systems (1.3) have at most one limit cycle.

(I) For the case $\alpha_L < 0$ and $\alpha_R < 0$. According to the statement (I) of Proposition 2.2, systems (1.3) have two finite equilibrium, P_L is an unstable focus and P_R is a saddle.

If $e^{\pi\gamma_L}V_+ + V_- > 0$, then systems (1.3) do not have either limit cycle or homoclinic connections by Theorem 3.1. We know that the two stable separatrices of the

saddle P_R cannot go together to the stable node E_1 at infinity, because one of the unstable separatrix of the saddle P_R would not has its $\omega-$limit set. So one of the stable separatrices of the saddle P_R goes to the unstable focus P_L and the other goes to the unstable node E_2 at infinity. Finally the two unstable separatrices of P_R have their $\omega-$limit sets at the unstable node E_2 at infinity. Thus the phase portrait of systems (1.3) is topologically equivalent to the one of Figure 2.1.

If $e^{\pi\gamma_L}V_+ + V_- < 0$, then systems (1.3) have a stable limit cycle which surround the focus P_L. Thus the stable separatrices of the saddle P_R goes to the unstable node E_2 at infinity, one of the unstable separatrices of the saddle P_R encircle the limit cycle and the other one goes to the stable node E_1 at infinity. Hence the phase portrait of systems (1.3) is topologically equivalent to the one of Figure 2.2.

If $e^{\pi\gamma_L}V_+ + V_- = 0$, then the unstable focus P_L is surrounded by a homoclinic orbit and there are no limit cycles. We know that the one of the stable separatrix of the saddle P_R and unstable separatrix must connect by continuity. The phase portrait of systems (1.3) is topologically equivalent to the one of Figure 2.3.

(II) For the case $\alpha_L < 0, \alpha_R = 0$. Systems (1.3) have two finite equilibrium: P_L is an unstable focus, and $O(0,0)$ is a boundary equilibrium, see Fig.3.1. It is obvious that systems (1.3) can not have limit cycles because the boundary equilibrium $O(0,0)$ has two invariant straight lines $y = (\gamma_R \pm 1)x$ in the region $x > 0$. Therefore the phase portrait of systems (1.3) is topologically equivalent to the one of Figure 2.4.

(III) For the case $\alpha_L < 0, \alpha_R > 0$. Systems (1.3) have one finite equilibrium P_L which is an unstable focus. Since $\alpha_R > 0$ systems (1.3) can not have limit cycles. Therefore the phase portrait of systems (1.3) is topologically equivalent to the one of Figure 2.5.

(IV) For the case $\alpha_L = 0, \alpha_R < 0$. Systems (1.3) have two finite equilibrium: P_R is a saddle, and $O(0,0)$ is a boundary equilibrium, see Fig.3.3.

If systems (1.3) have no limit cycles, then the two unstable separatrices of saddle P_R must go to the stable node E_1 at the infinity since $O(0,0)$ is an unstable focus. The stable separatrices of the saddle P_R have their α limit set at the unstable node E_2 and boundary equilibrium $O(0,0)$ respectively. Hence the phase portrait of systems (1.3) is topologically equivalent to the one of Figure 2.6.

If systems (1.3) have a unique limit cycle, its must stable and surround the boundary equilibrium $O(0,0)$. It is obvious that both of the stable separatrices of saddle P_R have their α limit sets at the unstable node E_2. And one of the unstable separatrix of the saddle P_R goes to the stable node E_1 at infinity, the other one encircle the stable limit cycle. Thus the phase portrait of systems (1.3) is topologically equivalent to the one of Figure 2.7.

From the above analysis, we know that the one of the stable separatrix of the saddle P_R and unstable separatrix must connect by continuity. Note that limit cycle and homoclinic connection can not coexist. Therefore the phase portrait of systems (1.3) is topologically equivalent to the one of Figure 2.8.

(V) For the case $\alpha_L = 0, \alpha_R = 0$. Systems (1.3) have a unique equilibrium $O(0,0)$ which is a boundary equilibrium, see Fig.3.2. It is obvious that systems (1.3) have

no limit cycles. Hence the phase portrait of systems (1.3) is topologically equivalent to the one of Figure 2.9.

(VI) For the case $\alpha_L = 0, \alpha_R > 0$. Systems (1.3) have a unique boundary equilibrium $O(0,0)$, see Fig.3.4. Note that systems (1.3) have no limit cycles because $\alpha_R > 0$. Thus the phase portrait of systems (1.3) is topologically equivalent to the one of Figure 2.10.

(VII) For the case $\alpha_L > 0, \alpha_R < 0$. Systems (1.3) have a unique saddle P_R. The origin $O(0,0)$ is a invisible two-fold singularity.

If $O(0,0)$ is stable and systems (1.3) have no limit cycles, then both of the stable separatrices of the saddle P_R have their α limit sets at the unstable node E_2 at infinity, and the unstable separatricies of the saddle P_R go to $O(0,0)$ and infinity stable node E_1, respectively. Therefore the phase portrait of systems (1.3) is topologically equivalent to the one of Figure 2.11.

If $O(0,0)$ is stable and systems (1.3) have a unique limit cycle, then both of the unstable separatrices of the saddle P_R have their ω limit sets at the unstable node E_1 at infinity, and the stable separatricies of the saddle P_R have their α limit sets at the infinity unstable node E_2 and the unstable limit cycle, respectively. Therefore the phase portrait of systems (1.3) is topologically equivalent to the one of Figure 2.13.

The phase portrait of Figure 2.12 can be obtained by the continuity of Figure 2.11 and Figure 2.13.

If $O(0,0)$ is unstable and systems (1.3) have no limit cycles, then both of the unstable separatrices of the saddle P_R have their ω limit sets at the stable node E_1 at infinity, and the stable separatricies of the saddle P_R go to $O(0,0)$ and infinity unstable node E_2, respectively. Therefore the phase portrait of systems (1.3) is topologically equivalent to the one of Figure 2.14.

If $O(0,0)$ is unstable and systems (1.3) have a unique limit cycle, then both of the stable separatrices of the saddle P_R have their α limit sets at the unstable node E_2 at infinity. One of the unstable separatrix of the saddle P_R goes to the infinity stable node E_1, and the other ones encircle the stable limit cycle. So the phase portrait of systems (1.3) is topologically equivalent to the one of Figure 2.16.

The phase portrait of Figure 2.15 can be obtained by the continuity of Figure 2.14 and Figure 2.16.

(VIII) For the case $\alpha_L > 0, \alpha_R = 0$. Systems (1.3) have a unique boundary equilibrium $O(0,0)$, see Figure 3.2. The phase portrait of systems (1.3) is topologically equivalent to the one of Figure 2.17.

(IX) For the case $\alpha_L > 0, \alpha_R > 0$. Systems (1.3) have no finite equilibrium. The phase portrait of systems (1.3) is topologically equivalent to the one of Figure 2.18. □

4.2. $\gamma_R \geqslant 0$.

Proposition 4.2. *The phase portrait of refracting systems (2.1) with $\gamma_L > 0$ and $\gamma_R \geqslant 0$ is topologically equivalent to*

(I) *Fig.2.1 if* $\alpha_L < 0$ *and* $\alpha_R < 0$*;*
(II) *Fig.2.4 if* $\alpha_L < 0$ *and* $\alpha_R = 0$*;*
(III) *Fig.2.5 if* $\alpha_L < 0$ *and* $\alpha_R > 0$*;*
(IV) *Fig.2.6 if* $\alpha_L = 0$ *and* $\alpha_R < 0$*;*
(V) *Fig.2.9 if* $\alpha_L = 0$ *and* $\alpha_R = 0$*;*
(VI) *Fig.2.10 if* $\alpha_L = 0$ *and* $\alpha_R > 0$*;*
(VII) *the ones of Fig.2.11 or Fig.2.14 if* $\alpha_L > 0$ *and* $\alpha_R < 0$*;*
(VIII) *Fig.2.17 if* $\alpha_L > 0$ *and* $\alpha_R = 0$*;*
(IX) *Fig.2.18 if* $\alpha_L > 0$ *and* $\alpha_R > 0$*.*

Proof. Recall that systems (1.3) have no limit cycles and homoclinic connections since $\gamma_L\gamma_R \geqslant 0$, the proof of Proposition 4.2 similar with Proposition 4.1. □

5. Acknowledgements

The first author is partially supported by the Natural Science Foundation of Guangdong Province (2017A030313010) and Science and Technology Program of Guangzhou (No. 201707010426).

The second author is supported by the Ministerio de Economía, Industria y Competitividad, Agencia Estatal de Investigación grants MTM2016-77278-P (FEDER) and MDM-2014-0445, the Agència de Gestió d'Ajuts Universitaris i de Recerca grant 2017SGR1617, and the H2020 European Research Council grant MSCA-RISE-2017-777911.

References

[1] J.C. Artés, J.Llibre, N.Vulpe, Quadratic systems with a polynomial first integral: A complete classification in the coefficient space $\mathbb{R}^2$, J. Differential Equations **246** (2009), 3535–3558.
[2] J.C.Artés, A.C.Rezende, R.D.S.Oliveira, Global phase portraits of quadratic polynomial differential systems with a semi-elemental triple node, Internat. J. Bifur. Chaos **23** (2013), 1350140, 21pp.
[3] M.di Bernardo, C.J.Budd, A.R.Champneys and P.Kowalczyk, Piecewise-Smooth Dynamical Systems, Applied Mathematical Sciences, Vol. 163, Springer-Verlag, London, (2008).
[4] M.Biák, T.Hanus, D.Janovska, Some applications of Filippov's dynamical systems, J. Comput. Appl. Math. **254** (2013), 132-143.
[5] C.A.Buzzi, J.C.R.Medrado and M.A.Teixeira, Generic bifurcation of refracted systems, Adv. Math. **234** (2013), 653–666.
[6] L.Cairó and J.Llibre, Phase portraits of planar semi-homogeneous vector fields (I), Nonlinear Anal. **29** (1997), 783–811.
[7] L. Cairó, J.Llibre, Phase portraits of planar semi-homogeneous vector fields (II), Nonlinear Anal. **39** (2000), 351–363.
[8] F.Cao, J.Jiang, The Classification on the Global Phase Portraits of Two-dimensional Lotka-Volterra System, J. Dyn. Diff. Equat. **20** (2008), 797–830.
[9] M.Caubergh, J.Llibre, J. Torregrosa, Global phase portraits of some reversible cubic centers with collinear or infinitely many singularities, Internat. J. Bifur. Chaos **22** (2012), 1250273, 20pp.
[10] H.Chen, S.Duan, Y.Tang and J.Xie, Global dynamics of a mechanical system with dry friction, J. Differential Equations **265** (2018), 5490–5519.
[11] B.Coll, A.Ferragut and J.Llibre, Phase portraits of the quadratic systems with a polynomial inverse integrating factor, Internat. J. Bifur. Chaos **19** (2009), 765–783.
[12] F.Dumortier, J.Llibre and J.C.Artés, Qualitative Theory of Planar Differential Systems, Springer-Verlag, Berlin Heidelberg, (2006).

[13] E.Freire, E.Ponce, F.Rodrigo and F.Torres, Bifurcation sets of continuous piecewise linear systems with two zones, Internat. J. Bifur. Chaos **8** (1998), 2073–2097.
[14] E.Freire, E.Ponce and F.Torres, Canonical discontinuous planar piecewise linear systems, SIAM J. Appl. Dyn. Syst. **11** (2012), 181–211.
[15] A.Guillamon and C.Pantazi, Phase portraits of separable Hamiltonian systems, Nonlinear Anal. 74 (2011), 4012–4035.
[16] S.Huan and X.Yang, Existence of limit cycles in general planar piecewise linear systems of saddle-saddle dynamics, Nonlinear Anal. **92** (2013), 82–95.
[17] S.Huan and X.Yang, On the number of limit cycles in general planar piecewise linear systems of node-node types, J. Math. Anal. Appl. **411** (2014), 340–353.
[18] J.Itikawa and J.Llibre, Global phase portraits of uniform isochronous centers with quadratic homogeneous polynomial nonlinearities, Discrete Contin. Dyn. Syst. Ser. B **21** (2016), 121–131.
[19] S.Li and J.Llibre, Phase portraits of piecewise linear continuous differential systems with two zones separated by a straight line, J. Differential Equations **266** (2019), 8094–8109.
[20] J.Llibre, Y.P.Martinez and C.Vidal, Phase portraits of linear type centers of polynomial Hamiltonian systems with Hamiltonian function of degree 5 of the form $H = H_1(x) + H_2(y)$, Discrete Contin. Dyn. Syst. **39** (2019), 75–113.
[21] J.Llibre, D.D.Novaes and M.A.Teixeira, Limit cycles bifurcating from the periodic orbits of a discontinuous piecewise linear differential center with two zones, Internat. J. Bifur. Chaos **25** (2015), 1550144, 11pp.
[22] J.Llibre, M.A.Teixeira and J.Torregrosa, Lower bounds for the maximum number of limit cycles of discontinuous piecewise linear differential systems with a straight line of separation, Internat. J. Bifur. Chaos **23** (2013), 1350066, 10pp.
[23] R.Lum and L.O.Chua, Global properties of continuous piecewise-linear vector fields. Part I: Simplest case in $\mathbb{R}^2$, Internat. J. Circuit. Theory Appl. **19** (1991), 251–307.
[24] J.C.Medrado and J.Torregrosa, Uniqueness of limit cycles for sewing planar piecewise linear systems, J. Math. Anal. Appl. **431** (2018), 529–544.
[25] Y.P.Martínez and C.Vidal, Classification of global phase portraits and bifurcation diagrams of Hamiltonian systems with rational potential, J. Differential Equations **261** (2016), 5923–5948.
[26] E.Ponce, J.Ros and E.Vela, The boundary focus-saddle bifurcation in planar piecewise linear systems. Application to the analysis of meristor oscillators, Nonlinear Anal. Real World Appl. **43** (2018), 495–514.
[27] J.Wang, X.Chen and L.Huang, The number and stability of limit cycles for planar piecewise linear systems of node-saddle type, J. Math. Anal. Appl. **469** (2019), 405–427.
[28] J.Wang, C.Huang and L.Huang, Discontinuity-induced limit cycles in a general planar piecewise linear system of saddle-focus type, Nonlinear Anal. Hybrid Syst. **33** (2019), 162–178.
[29] L.Zhu, Dynamics of switching van der Pol circuits, Nonlinear Dyn. **87** (2017), 1217–1234.

[1] School of Mathematics and Statistics, Guangdong University of Finance and Economics, Guangzhou, 510320, P.R. China

Email address: lism1983@126.com

[2] Departament de Matemàtiques, Universitat Autònoma de Barcelona, 08193 Bellaterra, Barcelona, Catalonia, Spain

Email address: jllibre@mat.uab.cat